Charge Trapping by Self-Assembled Monolayers as the Origin of the Threshold Voltage Shift in Organic Field-Effect Transistors

Gholamrezaie, Fatemeh; Andringa, Anne-Marije; Roelofs, W. S. Christian; Neuhold, Alfred; Kemerink, Martijn; Blom, Paul W. M.; de Leeuw, Dago M.

Published in:
Small

DOI:
10.1002/smll.201101467

Publication date:
2012

Charge Trapping by Self-Assembled Monolayers as the Origin of the Threshold Voltage Shift in Organic Field-Effect Transistors

Fatemeh Gholamrezaie, Anne-Marije Andringa, W. S. Christian Roelofs, Alfred Neuhold, Martijn Kemerink, Paul W. M. Blom, and Dago M. de Leeuw**

Application of organic TFTs is envisioned in pixel engines in active matrix displays and in integrated circuits for contactless radio-frequency identification transponders.[1–3] A key device parameter of a transistor is the threshold voltage, V_{th}. This voltage should be set at a given value and, furthermore, be identical for all devices in a circuit. Any deviation yields a reduced gain of logic gates, a decreased noise margin of integrated circuits or an inhomogeneously emitting display.[4,5] For standard Si transistors, the threshold voltage can be accurately set by the amount of doping applied by ion implantation.[6,7] In organic transistors, however, local doping of individual transistors is not an option. To get around this constraint and to externally set V_{th}, several options have been published, such as the incorporation of level shifters in integrated circuits,[8] the use of a gate metal with a specific work function,[9,10] or the use of dual-gate transistors.[11] As an alternative method, the application of a self-assembled monolayer (SAM) at the gate dielectric interface has been reported.[12–16] The threshold voltage can be set by varying the chemical composition of the SAM. The change in V_{th} has tentatively been explained as being due to the dipole moment of the composing molecules. Device simulations, however, have indicated that the dipolar contribution is too small.[17] Alternatively, trapped interface charges have been suggested. The mechanism is under debate; as mentioned in a recent publication direct experimental evidence to accurately explain the voltage shifts is still lacking.[16]

Here we fabricated organic field-effect transistors with various self-assembled monolayers on the gate dielectric. The value of the threshold voltage varies over tens of volts, depending on the nature of the SAM. To elucidate the origin of the significant differences, the semiconductor was peeled off, and the surface potential of the SAM-modified gate dielectric was measured by scanning Kelvin-probe microscopy (SKPM).[18,19] We unambiguously show that the origin of the threshold voltage shifts is the charge trapping induced by the SAM. The temporal behavior of the surface potential after removing the semiconductor is discussed.

Transistor test devices were fabricated as described in the Experimental Section. Three types of organosilane molecules with ethoxy end groups were used, viz. $(CF_3)(CF_2)_7(CH_2)_2Si(OC_2H_5)_3$, $(CH_3)(CH_2)_9Si(OC_2H_5)_3$, and $(NH_2)(CH_2)_3Si(OC_2H_5)_3$. The corresponding SAMs will be referred to as CF_3-, CH_3- and F-SAM, respectively. The chemical structures are presented as insets in **Figure 1**. The microstructure of the SAMs was investigated with X-ray reflectivity, contact angle, and atomic force microscopy (AFM) measurements. Figure 1 shows the reflected X-ray intensity as a function of incidence angle. The fully drawn curves are a fit to the data. The calculated and measured values of the SAM thickness are presented in **Table 1**. The values agree with the calculated lengths of the molecules. Only in case of the NH_2-SAM the numbers deviate, which could be due to formation of a double layer. The hydrophobicity of the SAMs was investigated by water contact angle measurements. The static contact angles presented in Table 1 correspond to literature values.[12,20,21] The morphology of the SAMs was investigated with AFM. A typical topographical image is presented in the inset of Figure 1. The monolayer is homogeneous without microscopic defects.

Saturated transfer curves of the polytriarylamine (PTAA) transistors with three different SAMs are presented in **Figure 2**a. The charge carrier mobility is in the order of 10^{-4}–10^{-3} $cm^2\ V^{-1}\ s^{-1}$. The major difference between the transistors is the value of the threshold voltage, here approximated by the pinch-off voltage. The offset between the pinch-off

F. Gholamrezaie, A. Andringa, Prof. P. W. M. Blom, Prof. D. M. de Leeuw
Molecular Electronics
Zernike Institute for Advanced Materials
University of Groningen
Nijenborgh 4, 9747 AG Groningen, The Netherlands
E-mail: fatemeh.gholamrezaie@philips.com; dago.de.leeuw@philips.com

F. Gholamrezaie, A. Andringa, W. S. C. Roelofs, Prof. D. M. de Leeuw
Philips Research Laboratories
High Tech Campus 4, 5656 AE Eindhoven, The Netherlands

W. S. C. Roelofs, Dr. M. Kemerink
Applied Physics
Eindhoven University of Technology
P.O. Box 513, 5600 MB Eindhoven, The Netherlands

A. Neuhold
Institute of Solid State Physics
Graz University of Technology
Petersgasse 16A, 8010 Graz, Austria

Prof. P. W. M. Blom
Holst Centre/TNO
High Tech Campus 34, 5656 AE, Eindhoven, The Netherlands

DOI: 10.1002/smll.201101467

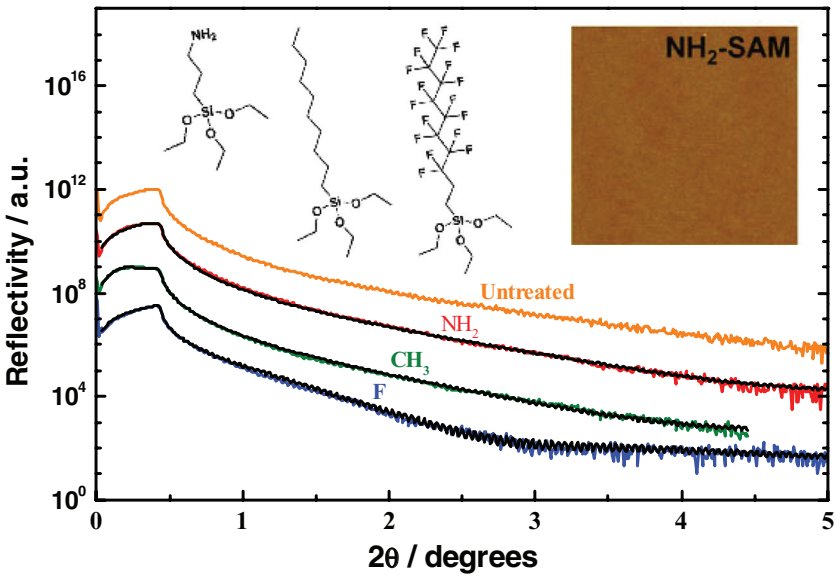

Figure 1. SAM characterization. X-ray reflection as a function of the diffracted angle for the SAMs. The solid black lines are fits to the experimental data. Inset: Chemical structures of the SAM molecules: NH_2-SAM, CH_3-SAM, F-SAM (from left to right). AFM topography image of 20 μm × 20 μm of NH_2-SAM (right).

voltage and the threshold voltage can be disregarded for the discussion. The threshold voltage of transistors with a CH_3-SAM is around 0 V; with a NH_2-SAM the threshold voltage is negative, and with a F-SAM the threshold voltage is positive. For the example of Figure 2a, the numbers are about 0, –16, and +20 V, respectively, in agreement with threshold voltages reported for corresponding pentacene transistors.[12]

The change in threshold voltage can be the result of the following mechanisms: the macroscopic dipole moment of the SAM, charge trapping at the gate dielectric semiconductor interface, or doping of the semiconductor. To disentangle the mechanisms, the local potential is probed with SKPM. The bulk semiconductor however electrically shields the buried SAM, which prevents the SAM from being probed directly; therefore the semiconductor has to be removed. With a piece of adhesive tape, the PTAA semiconductor layer is completely removed as a continuous film from the gate dielectric. After peeling off the polymer, the source–drain current is zero. The exfoliation is facilitated by the SAM, which lowers the interfacial energy. The complete removal is supported by X-ray photoelectron spectroscopy (XPS) measurements, a well-established technique to identify the chemical composition of the top-most surface layers. Nitrogen is a marker for the presence of the semiconductor PTAA. **Figure 3** presents the N 1s peak with a binding energy around 399 eV before and after exfoliation of the PTAA. For the F-SAM and the CH_3-SAM, the signal has completely disappeared as checked on various spots on the surface, indicating the complete removal of PTAA. For the NH_2-SAM, XPS is not an appropriate technique because nitrogen is present in both the polymer and monolayer. Contact angle measurements confirm that the SAM itself is not affected by exfoliation. Table 1 shows that the static contact angles after peeling off the SAM resemble the contact angles before peeling off. A photograph of the CH_3-SAM contact angle after exfoliation is presented as an inset in Figure 3.

Table 1. Thickness of the SAMs derived from X-ray reflectivity measurements and calculated length of the molecules. Static contact angles of the SAMs before and after exfoliation of the PTAA semiconductor are presented.

	F-SAM	CH_3-SAM	NH_2-SAM
SAM thickness [nm]	1.3	1.1	0.88
SAM thickness caculated [nm]	1.2	1.2	0.36
Water contact angle [°]	108	91	67
Water contact angle after exfoliation [°]	105	90	64

The surface potential of the area between the source and drain, i.e., the channel region, was measured as quickly as possible after measuring the transfer curve (Figure 2a) and peeling off the PTAA layer. During the SKPM measurement, all electrodes were grounded. The local surface potentials are presented in Figure 2b. The offset at the source and drain contacts is due to the capacitive coupling between the AFM cantilever and the transistor channel region. The surface potential in the channel region depends on the type of SAM. For the CH_3-SAM the surface potential is zero. In the case of the F-SAM, a negative surface potential of –18 V is observed while the NH_2-SAM shows a positive surface potential of +14 V.

The surface potentials have been measured as fast as possible after peeling off because their amplitude decreases with time. As an example the temporal behavior of the F-SAM is presented in **Figure 4**a. The value of the maximum potential is plotted as a function of time in Figure 4b. The potential decreases about exponentially with time. The time constant depends on the relative humidity of the air. At 60% relative humidity, the decay constant is a factor of five smaller than in dry air. The temporal behavior is not well understood. The trapped charges in the channel region become compensated, which might be caused by surface conduction of absorbed water.[22]

The threshold voltage of a field-effect transistor is equal to the flat band voltage, V_{FB}, corrected for fixed oxide charges, Q_f, trapped interface charges, Q_i,[23] and the dipolar contribution due to SAM, V_{SAM}. C is the capacitance.

$$V_{th} = V_{FB} + V_{SAM} - \frac{Q_f + Q_i}{C} \quad (1)$$

Flat band voltages are typically on the order of 0.1 V. The dipolar potential follows from the Helmholtz equation:

$$V_{SAM} = \frac{\mu_{zSAM}}{A\varepsilon_r\varepsilon_0} \quad (2)$$

where μ_{zSAM} is the net vertical component of the molecular dipole moment, A is the lateral area per molecule, ε_r is the

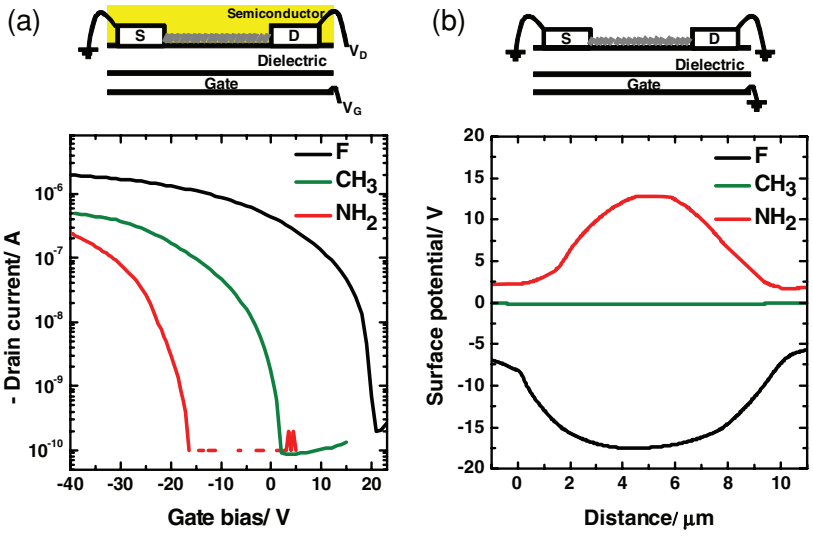

Figure 2. Electrical characterization. a) Saturated transfer characteristics of field-effect transistors with the three different SAMs on the gate dielectric. The black, green, and red lines correspond to the F-SAM, CH_3-SAM, and NH_2-SAM, respectively. The channel length and width are 10 and 10 000 µm, respectively, and the source–drain bias is −30 V. At the top the transistor layout is depicted schematically with the source (S), drain (D), and gate (G) electrodes. b) Local surface potentials of the SAMs after peeling off the PTAA semiconductor. The black, green, and red lines correspond to the F-SAM, CH_3-SAM, and NH_2-SAM, respectively. The transistor layout after delamination is schematically presented at the top. During SKPM measurements all electrodes are grounded.

relative permittivity of the molecule and ε_0 is the vacuum permittivity.[24] The surface potentials were measured directly after applying the SAM on the gate dielectric prior to applying the PTAA semiconductor. The local potentials as a function of position in the channel region are presented in the **Figure 5**. The surface potentials are on the order of about 1 V and might be due to a dipolar contribution of the ordered molecules. The values of the observed threshold voltages are too big to be a result of the dipole moment of the SAM. Reported device simulations confirm the small dipolar contribution of less than 1 V for molecules with comparable dipole moments.[17] All SAMs bind in the same manner to the SiO_2 surface. The transfer curve of the CH_3-SAM exhibits a threshold voltage around 0 V. Therefore, it is extremely unlikely that the observed variations in threshold voltage are due to fixed oxide charges. Hence the changes in threshold voltage of the NH_2-SAM and F-SAM are due to trapped interface charges. This assignment is confirmed by the SKPM measurements. The contributions to the surface potential of the dipole moment of the molecules, the flat band voltage, and the fixed charges can be neglected with respect to the contribution of the interface charges. Therefore the surface potential when using grounded electrodes is given by $V_{SKPM} \approx Q_i / C$; i.e. it is largely dominated by trapped interface charges.

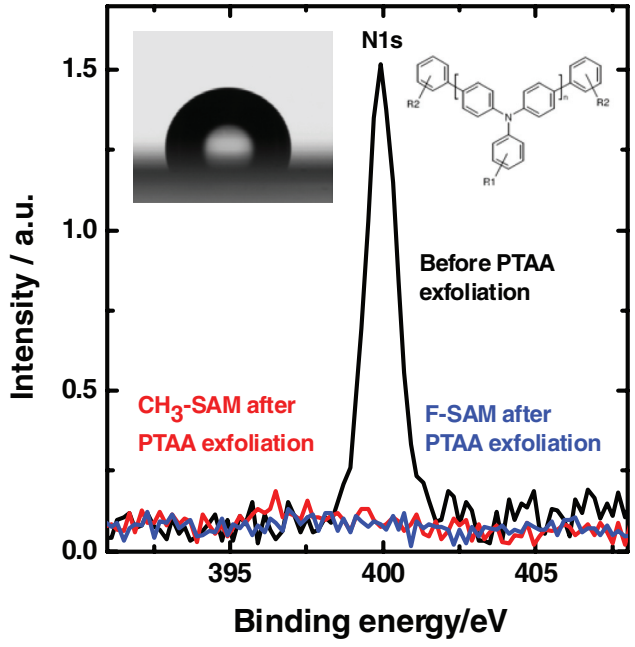

Figure 3. Exfoliation. X-ray photoelectron spectra before and after peeling off the PTAA semiconductor. The black line shows the PTAA N 1s peak before peeling off. The red line and blue line are measured after peeling off the PTAA semiconductor from the CH_3-SAM and F-SAM. The insets show the chemical structure of the PTAA semiconductor and a picture of a water droplet on the pristine CH_3-SAM.

In dry air the maximum surface potential of the stripped device extrapolated back to time zero perfectly matches with the corresponding threshold voltages (Figure 4b). In humid air the changes are too fast to reliably estimate the extrapolated starting potential. The agreement between extrapolated potential and threshold voltage unambiguously shows that the threshold voltage shift originates from trapped charges by the SAM. The CH_3-SAM is inactive while the NH_2-SAM traps positive charges and the F-SAM traps negative charges. The presence of the negative charges could be due to surface conduction of the SiO_2,[22] but it is not completely clear yet.

We note that it is well known that exfoliation of two insulating materials can yield static charges by contact electrification or tribo-charging. A review on space-charge electrets that exhibit a net macroscopic electrostatic charge has been presented in the literature.[25] The classical example is the charging of adhesive tape by unrolling. Peeling off ordinary sticky tape in vacuum can even yield individual X-ray pulses, typically a few nanoseconds long, of up to 15 kV.[26] However, the potentials measured here are not generated by the peeling process.

Firstly, the one-to-one correspondence between the threshold voltage shifts due to application of SAMs on the gate dielectric with the surface potentials as measured by SKPM would be a rare coincidence. The measured surface potentials are highly reproducible. That is not expected when the charges are generated by peeling off. Then a large spread in the amount of static charges is expected. Secondly, in separate series of experiments, the surface potentials were measured with KPM before and after peeling off adhesive

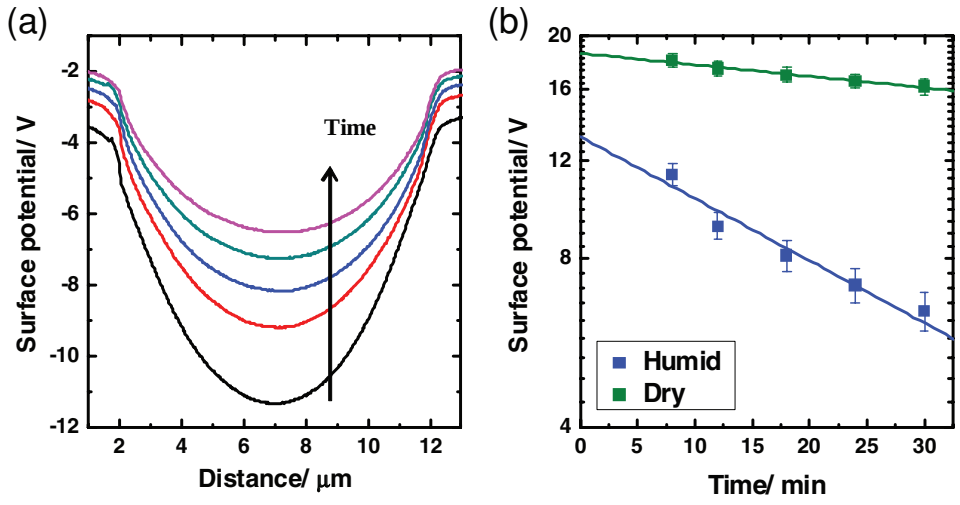

Figure 4. Temporal behavior of potential. a) Surface potential profiles measured with SKPM on the F-SAM after peeling off the PTAA semiconductor. The potentials decrease with time. The time interval between the measurements amounted to 6 min. The relative humidity was 60%. b) Maximum local surface potentials as a function of time. The green and blue points were measured in a relative humidity of 30% and 60%. The solid lines are an exponential fit to the data.

tape from a variety of substrates. Unrolling tape itself yields potentials higher than experimentally could be measured. Peeling off tape from a bare metal substrate does not lead to any static charges, as expected. Repetitive experiments on bare back-gated SiO_2 transistor substrates showed potential differences before and after exfoliation of at most 0.5 V. The measurements agree with literature data. Surface potentials of only 0.95 V were measured after peeling off Alq_3 with adhesive tape.[27] Thirdly, the exact same exfoliation procedure has been used previously to locate trapped charges in PTAA field-effect transistors generated upon prolonged application of the gate bias.[19] After stressing the threshold voltage was measured. Subsequently the semiconductor was peeled off with adhesive tape, and the surface potential of the revealed interface was measured using SKPM. A one-to-one correlation of the threshold voltage shift with the measured surface potential was found, ruling out that the static charges are generated in the peeling process. Finally, depending on the nature of the SAM the transistor is either normally-on or normally-off, meaning that at 0 V bias, the semiconductor is either conducting or insulating. In a normally-on transistor, exfoliation cannot generate stable static charges, and therefore, the experimental procedure cannot be the cause of the negative threshold voltage shift. In short, generation of static charges by the exfoliation process can be disregarded. The measured threshold voltage shifts are due to charges trapped by the SAM.

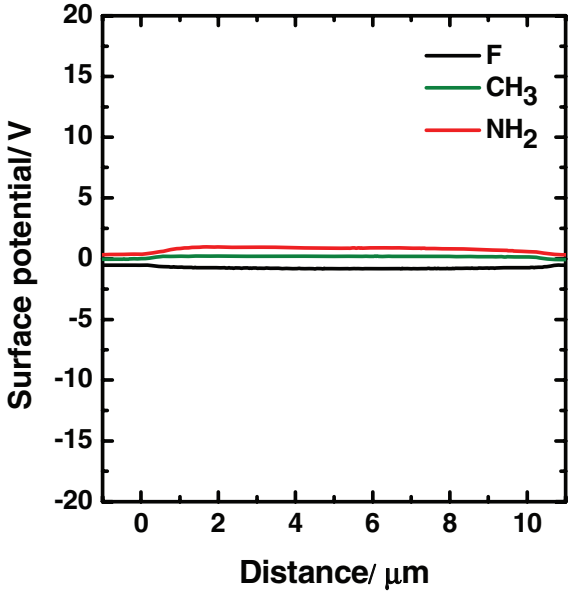

Figure 5. Local surface potentials in the channel region after applying SAMs on the gate dielectric, prior to depositing the PTAA semiconductor. The black, green, and red lines correspond to the F-SAM, CH_3-SAM, and NH_2-SAM, respectively.

In summary, we fabricated organic field-effect transistors with different self-assembled monolayers on the gate dielectric. The threshold voltage depends on the type of SAM. In agreement with literature data, the threshold voltage of CH_3-SAM is about 0 V, while the values for F-SAM and NH_2-SAM are at 20 and –16 V, respectively. To elucidate the origin of the large differences, the semiconductor was peeled off after electrical characterization, and the surface potential of the SAM modified gate dielectric was measured by SKPM. The surface potentials agree with the corresponding threshold voltage, which unambiguously shows that the surface potential shift is due to the charge trapping by the SAM.

Experimental Section

Transistor test devices were fabricated with heavily doped n^{++} Si monitor wafers acting as a common gate electrode with 200 nm thermally grown SiO_2 as gate dielectric. Au source and drain electrodes were defined using conventional photolithography. Ti was used as an adhesion layer. The test devices were treated for 10 min with UV-ozone to remove all organic compounds. Three

small NANO MICRO

types organosilane molecules with ethoxy end groups were used, viz. $(CF_3)(CF_2)_7(CH_2)_2Si(OC_2H_5)_3$, $(CH_3)(CH_2)_9Si(OC_2H_5)_3$, and $(NH_2)(CH_2)_3Si(OC_2H_5)_3$. The SAMs were grown by vapor deposition at 120°C for the NH_2-SAM and 150 °C for the CH_3-SAM and F-SAM. The treated test devices were rinsed with iso-propanol to remove noncovalently bound molecules. PTAA was used as a p-type amorphous semiconductor. The chemical structure is presented in Figure 3. Thin films were spin-coated from a toluene solution.

Specular X-ray reflectivity (XRR) measurements were performed using a X'Pert MRD pro diffractometer in the Bragg—Brentano geometry. The calculated fit to the XRR results is based on the recursive algorithm of Parratt and the roughness model of Nevot and Croce. XPS measurements were carried out using monochromatic Al Kα-radiation in a Quantera SXM from Ulvac-PHI. AFM measurements were conducted with a Veeco Dimension 3100 atomic force microscope equipped with a Nanoscope IV control unit. SKPM measurements were performed in ambient atmosphere. The height profile was recorded in tapping mode. The potential profiles were scanned in noncontact-lift mode 20 nm above the surface. Water contact angles were measured with a Contact Angle System OCA 30. The electrical transport was characterized using a HP 4155C semiconductor parameter analyzer.

Acknowledgements

We gratefully acknowledge R. Resel from Graz University of Technology, Austria and S. G. J. Mathijssen from the Technical University Eindhoven for fruitful discussions, and T. C. T. Geuns, H. J. Wondergem, and C. van der Marel from MiPlaza, Eindhoven for technical assistance. We acknowledge financial support from the Dutch Polymer Institute, project 624 and from the European project ONE-P, no. 212311.

[1] G. H. Gelinck, H. E. A. Huitema, E. Van Veenendaal, E. Cantatore, L. Schrijnemakers, J. B. P. H. Van der Putten, T. C. T. Geuns, M. Beenhakkers, J. B. Giesbers, B. H. Huisman, E. J. Meijer, E. M. Benito, F. J. Touwslager, A. W. Marsman, B. J. E. Van Rens, D. M. De Leeuw, *Nat. Mater.* **2004**, *3*, 106.

[2] E. Cantatore, T. C. T. Geuns, G. H. Gelinck, E. van Veenendaal, A. F. A. Gruijthuijsen, L. Schrijnemakers, S. Drews, D. M. de Leeuw, *IEEE J. Solid St. Circ.* **2007**, *42*, 84.

[3] K. Myny, S. Steudel, P. Vicca, M. J. Beenhakkers, N. van Aerle, G. H. Gelinck, J. Genoe, W. Dehaene, P. Heremans, *Solid St. Elect.* **2009**, *53*, 1220.

[4] S. De Vusser, J. Genoe, P. Heremans, *IEEE Trans. Elect. Dev.* **2006**, *53*, 601.

[5] J. R. Hauser, *IEEE Trans. Educ.* **1993**, *36*, 363.

[6] M. R. MacPherson, *Appl. Phys. Lett.* **1971**, *18*, 502.

[7] T. Mizuno, J. Okamura, A. Toriumi, *IEEE Trans. Elect. Dev.* **1994**, *41*, 2216.

[8] E. Cantatore, T. C. T. Geuns, G. H. Gelinck, E. van Veenendaal, A. F. A. Gruijthuijsen, L. Schrijnemakers, S. Drews, D. M. de Leeuw, *IEEE J. Solid St. Circ.* **2007**, *42*, 84.

[9] I. Nausieda, K. K. Ryu, D. Da He, A. I. Akinwande, V. Bulovic, C. G. Sodini, *IEEE Trans. Elect. Dev.* **2010**, *57*, 1003.

[10] H. W. Zan, W. T. Chen, C. C. Yeh, H. W. Hsueh, C. C. Tsai, H.F. Meng, *Appl. Phys. Lett.* **2011**, *98*, 153506.

[11] M. Spijkman, E. C. P. Smits, P. W. M. Blom, D. M. de Leeuw, Y. B. S. Côme, S. Setayesh, E. Cantatore, *Appl. Phys. Lett.* **2008**, *92*, 143304.

[12] S.Kobayashi, T. Nishikawa, T. Takenobu, S. Mori, T. Shimoda, T. Mitani, H. Shimotani, N. Yoshimoto, S. Ogaw, Y. Iwasa, *Nat. Mater.* **2004**, *3*, 317.

[13] K. P. Pernstich, S. Haas, D. Oberhoff, C. Goldmann, D. J. Gundlach, B. Batlogg, A. N. Rashid, G. Schitter, *J. Appl. Phys.* **2004**, *96*, 6431.

[14] Y. Jang, J. H. Cho, D.H. Kim, Y. D. Park, M. Hwang, K. Cho, *Appl. Phys. Lett.* **2007**, *90*, 132104.

[15] J. Takeya, T. Nishikawa, T. Takenobu, S. Kobayashi, Y. Iwasa, T. Minani, C. Goldmann, C. Krellner, B. Batlogg, *Appl. Phys. Lett.* **2004**, *85*, 5078.

[16] Y. Chung, E. Verploegen, A. Vailionis, Y. Sun, Y. Nishi, B. Murmann, Z. Bao, *Nano Lett.* **2011**, *11*, 1161.

[17] S. K. Possanner, K. Zojer, P. Pacher, E. Zojer, F. Schürrer, *Adv. Funct. Mater.* **2009**, *19*, 958.

[18] V. Palermo, M. Palma, P. Samori, *Adv. Mater.* **2006**, *18*, 145.

[19] S. G. J. Mathijssen, M. J. Spijkman, A. M. Andringa, P. A. van Hal, I. McCulloch, M. Kemerink, R. A. J. Janssen, D. M. de Leeuw, *Adv. Mater.* **2010**, *22*, 5105.

[20] H. Sugimura, K. Ushiyama, A. Hozumi, O. Takai, *Langmuir* **2000**, *16*, 885.

[21] A. Hozumi, Y. Yokogawa, T. Kameyama, H. Sugimura, K. Hayashi, H. Shirayama, O. Takai, *J. Vac. Sci. Technol. A* **2001**, *19*, 1812.

[22] S. G. J. Mathijssen, M. Kemerink, A. Sharma, M. Cölle, P. A. Bobbert, R. A. J. Janssen, D. M. de Leeuw, *Adv. Mater.* **2008**, *20*, 975

[23] S. M. Sze, *Physiscs of Semiconductor Devices*, Wiley-Interscience, New York **1981**.

[24] D. J. Ellison, B. Lee, V. Podzorvo, C. D. Frisbie, *Adv. Mater* **2011**, *23*, 502.

[25] L. S. McCarty, G. M. Whitesides, *Angew. Chem. Int. Ed.* **2008**, *47*, 2188.

[26] C. G. Camara, J. V. Escobar, J. R. Hird, S. J. Putterman, *Nature* **2008**, *455*, 1089.

[27] Y. Okabayashi, E. Ito, T. Isoshima, H. Ito, M. Haraet, *Thin Solid Films* **2009**, *512*, 839.

Received: July 20, 2011
Revised: September 26, 2011
Published online: November 25, 2011